International Research Journal of Engineering and Technology (IRJET) e-ISSN: 2395-0056
Volume: 09 Issue: 06 | June 2022 www.irjet.net p-ISSN: 2395-0072

Study of Geo-Spatial Data Quality

Aman Srivastava [1], Dr Shudhakar Shukla [2], Dr Anurag Ohri [3]

[1] *M.Tech Scholar, School Of Geoinformatics, Remote Sensing Application Centre, Uttar Pradesh, India.*
[2] *Scientist-SE School Of Geoinformatics, Remote Sensing Application Centre, Uttar Pradesh,India.*
[3] *Dr. Anurag Ohri Associate Professor Department of Civil Engineering, IIT (BHU)*

Abstract - The National Standard for Spatial Data Accuracy describes a way to measure and report positional accuracy of features found within a geographic data set. Approved in 1998, the NSSDA recognizes the growing need for digital spatial data and provides a common language for reporting accuracy. Data Quality provides information on, and a general assessment of, the quality of a data set or information resource. Positional accuracy has always been considered a defining and essential element of the quality of any cartographic product as it affects factors such as geometry ,topology, thematic quality and it directly related to the interoperability of spatial data. This study aims to produce accurate geospatial 3D data from unmanned aerial vehicles(UAV) images. An image of a approx. 5.26 km^2 area of the Banaras Hindu University campus in Varanasi ,Uttar Pradesh India, was captured using a DJI Mavic Pro Platinum drone. Arc GIS pro and Pix4dmapper programs were used to generate the solution. The horizontal and vertical accuracies were obtained with UAV solution. The root mean square error (RSME) was calculated of some points. The analysis of the points of horizontal and vertical points were done as well as the accuracy error shown in the tabulated form.

Key Words: Unmanned aerial vehicles(UAV), Photogrammetry, GPS, Root Mean Square Error(RSME)

1. INTRODUCTION

In the past, the use of unmanned aerial vehicles (UAVs) or drones was primarily motivated by military goals and applications. Three decades ago, UAVs were first used in geomatics applications, but today they have become a commonly used tool for data acquisition. This technique provides a low-cost alternative to classical aerial photogrammetry of small areas and large-scale topographic mapping or detailed 3D surface information. UAVs also have civilian applications, such as pesticide spraying in agriculture to prevent health problems and documenting building facades and archeological site. For photogrammetric mapping applications, many researchers have used UAV platforms for geomatics applications, instead of traditional photogrammetric methods, to produce digital surface models (DSM) or digital terrain models (DTMs). For example, UAV platforms have been used to investigate coastal applications in Ghana for monitoring beach sediment volume dynamics and to create 3D models of complex structures, such as masonry bridges. The effects of different flight directions and heights on the UAV image bundle block adjustment (BBA) were investigatedby Gerke and Przybilla. Further, a review of UAV technology for photogrammetry and remote sensing applications, with an emphasis on regulations, acquisition systems, navigation, and orientation, is presented in Colomina and Molina.There are two methods to align or geo-reference data: direct and indirect methods. Direct geo-referencing can be achievedusing the camera position information of a global navigationsatellite system (GNSS), recorded by the onboard receiver during UAV flight. There is time synchronization between thecamera and GPS of a UAV system. The first approximation of the camera position is calculated using the GNSS onboard the UAV. The SIFT algorith is then used to detecta large number of features that can be used as tie/pass pointsinside the overlapped areas between adjacent images to refinethe geo-reference solution. Although this method is faster and more economical, it provides low solution quality and isnot recommended for high-precision applications, such as documentation of historical buildings or industrial applications.The indirect geo-referencing method can be applied using thecoordinates of certain targets as ground coordinate points(GCPs). These targets must be clearly visible and distinguish- able in the images for manual selection of their centers duringthe data processing steps. It is also possible to use any existingartificial features in an environment that are fixed, such as corners, manhole covers, or road markings. Preparing and measuring the positions of GCPs requires time and effort, but this method is preferred if a higher-precision product is required.

Researchers have investigated UAV data not only in terms of their accuracy but also with respect to six challenges that apply to small UAVs in remote sensing: hostile flying environments, power constraints, available sensors, payload weight, data analysis, and regulation. Many researchers have con- ducted field tests to determine the accuracy of UAV data col- lection techniques. In the current study, accuracy is defined as how close the measured position of a pixel is in relation to its true position. Using UAV photogrammetry, point clouds with an absolute point position accuracy of approximately

20 cm were obtained, making this method suitable for topographic surveys. Without using GCPs, the real time kinematic (RTK) solution consistently achieves a root-mean-square error (RMSE) between 2 and 3 cm for the horizontal accuracy of used checkpoints (CPs), while the obtained vertical accuracy was between 2 and 10 cm. Four different software packages (Arc-Gis Pro, SimActive Correlator3D, BentleyContext Capture, and Pix4D) were used to investigate 3D information obtained from UAV photogrammetry [7,14]. The results show that the 3D RMSE ranges from 0.54 to 0.06 m. Two case studies were carried out using the UAV sys- tem to calculate horizontal and vertical accuracy. In the first case study, the radial horizontal and vertical RMSE were calculated as 0.05 m and 0.06 m, respectively; for the second case study, these values were 0.08 m and 0.03 m, respectively. A comparison was made between the digital elevation models (DEMs) obtained with a UAV system and the total station observation method. ArcGis Pro was used to process approx. 135 images captured using a UAV system. The obtained mean average error of GCPs was 0.043 m for the geo-referenced process, and the RMSE value for the CPs was 4.79 cm. In real-life applications, such as construction sites, 64 photos of a test area were captured with a UAV system (camera with 16 mm focal length and 16.1 megapixels per image) with a ground resolution of 2 cm per pixel. The estimated mean errors were 2 cm (horizontal) and 6 cm (vertical). Oniga et al. imaged an area of nearly 1 ha with DJI Phantom 3 at two flying heights (28 m and 35 m) to determine the optimum numberof GCPs required for the indirect geo-referencing process to produce highly accurate results. Their results indicated that an error of 7 cm can be obtained using pix4dmapper software with 32 GCPs, while 8.4 cm is the minimum error for 3DF Zephyr Pro software with 19 GCPs. Crydermanetal. compared the stockpile volumetric surveys obtained with a UAV system and RTK GPS observations; both stockpile volumeresults agreed within 0.7%. In another accuracy assessment of UAV photogrammetry, 160 photos of a 17.64 ha projectarea were captured by UAV with a flying height of 120 m, and the number of GCPs during the geo-referencing process was varied. Using 15 GCPs, the optimal horizontal accuracy $RMSE_{xy}$ was 3.3 cm, and vertical accuracy $RMSE_z$, 5.8 cm. To test the system's accuracy, Barry and Coakley imaged a 2 ha site using a UAV at an altitude of 90 m to pro-vide an expected ground sampling distance (GSD) of 10 mm.A total of 10 GCPs were used during geo-referencing, and 45 CPs were used to assess accuracy. They obtained accuracies of 2.3 cm and 3.5 cm for the $RMSE_z$ and $RMSE_{xy}$, respectively.The general aim of this study is to assess the feasibility of using low-cost DJI Mavic Pro UAV to obtain accurate 3D spatial data for large-scale maps. The first objective is to quan tify the increase in accuracy achieved by using some GCPs versus no GCPs. The second objective is to compare different image processing packages to obtain point-cloud information using this system. Two software packages, ArcGis Pro Professional version 1.5.2 and Pix4dmapper, were chosen to calculate the mathematical solution for the study area. Thepaper first describes the study area, UAV system, flight planning, and GCP coordinate collection methods. The subsequent sections introduce the proposed processing method and dis- cusses the results of the experiment along with the accuracyof the obtained models, drawing comparisons between the different software packages. The final section concludes the work.

1.1 Data Quality Measures

Table1:Data Quality Measures

Category	Sub-category
Completeness	Commission
	Omission
Consistency	Conceptual
	Domain
	Format
	Topological
Positional Accuracy	Absolute or External
	Gridded data
Temporal Quality	Accuracy of a time measurement
	Temporal consistency
	Temporal validity
Thematic Accuracy	Classification correctness
	Non-quantitative attribute correctness
	Quantitative attribute accuracy
Aggregation Measures	Data product specification check

A total number of measures identified as sixty-one out of which twenty-six are observed as essential and thirty-five as optional parameters in the data quality assessment. However, the total number of parameters tested is completely depends on application and the data product specification provided by the organization.

1.2 Positional Accuracy Standards

Positional accuracy is the quantifiable value that represents the positional difference between two geospatial layers or between a geospatial layer and reality. To assess positional accuracy, two layers are required: the layer whose accuracy you want to evaluate and another layer that can be used as a point of reference. The uncertainty is defined as the circular error (CE) for two-dimensional features and linear error (LE) for three-dimensional features. The confidence level for

the feature class or raster being evaluated can be at the 90, 95, 98 or 99 percent level.

2. Description of the study area and the UAV system

2.1 Study area

2.2 UAV system

For our field test, the DJI Mavic Pro Platinum drone was used to image the test area. The first-generation Mavic Pro was released in 2016. The Mavic Pro Platinum model has a longer flight time of 30 min, and it is not designed to carry payloads. The flight time of a UAV is highly dependent on the flight speed and wind speed. Table 1 and Fig. 2 illustrate the charac- teristics of the UAV system used in this study. The drone was connected to a low-cost GPS receiver and magnetic compass.

Fig.1 DJI Mavic Pro Platinum drone equipped with RGB camera.

The inertial measurement unit (IMU) was used to obtain the actual alignment, acceleration, and barometric altitude. The total hardware cost of this system was estimated to be approximately $2000.

Fig.2 Study Area of Banaras Hindu University

2.3 Flight Planning And Image Acqusition

Before imaging the study area, a suitable flight plan that con- tains many variables, such as flight height, GSD, and total number of photos, was designed. The GSD influences the qual- ity of the final results and the details of the final orthomosaic.

$$GSD = \frac{S_w \times H \times 100}{F_r \times IM_w}$$

Equation:1

Here, Sw is the real sensor width (mm), Fr is the real focal length (mm), and IMwis the image width (px). For example, using a DJI Mavic Pro drone, a GSD of 2.3 cm/px can theo- retically be achieved at a flight height of 70 m. Eq. contains all flight parameters, and flight planning was conducted with Pix4Dcapture, a free mobile phone application for drone flight planning. Within this application, the user must specify several parameters, such as the area of interest, photograph overlap percentage, and flight height or desired GSD. By setting the end overlap and side overlap to 70% and 30%, respectively, the camera is oriented in a nadiral position. The flight was per- formed in a single grid mode to reduce the processing time using four strips. Fig. 3 shows the acquisition plan for the cap- tured images. Photographs that were of low quality or fuzzy, had tiny coverage areas, or were duplicated were excluded from the original set of photos. The resulting 36 images show- ing the best coverage were processed using different software packages.

3. Processing methodology

3.1From images to orthophotos

The captured images were processed using two software pack- ages: Agisoft Metashape and Pix4dmapper. An orthorectified image mosaic was generated after producing a point cloud from the photos using the structure-from-motion (SfM) calcu- lation method employed by both software packages. The stan- dard solution technique for photogrammetry is BBA; an introduction to the BBA is provided by Wolf and Dewitt

The SfM method differs from the photogrammetric method in its ability to calculate camera positions and their orientation parameters with or without GCPs. The SfM algorithm initially uses the scale invariant feature transform (SIFT) algorithm to collect and determine local features within each image . In this study, a complete review of the SfM method is not relevant, and the reader can refer to previous literature for a more detailed discussion. The processing steps are divided into three main parts: image alignment, con- struction of point clouds and mesh, and construction of DSM and orthophotos. Both software packages used in this study were fully automated. The user only needs to add the images, place markers, and define a few optional input param- eters, such as the project datum and projection, GCPs and CPs, and final resolutions. Thereafter, the camera alignment is optimized, and, finally, dense point clouds, DSMs, and orthomosaics are created.

3.2 Statistical analysis

Accuracy measures are based on the variation between the obtained UAV photogrammetry solution value and the refer- ence value at selected CPs. The reference values were collected by RTK GPS observations before the image-capturing step, and the RMSE was calculated from the differences. The RMSE is frequently used to measure the deviations between the reference data (more accurate) and UAV-derived data.

For the full analysis of the points which are taken is shown by the difference with the help of statistics t- test analysis.

The formula of the paired t-test is defined as the sum of the differences of each pair divided by the square root of n times the sum of the differences squared minus the sum of the squared differences, overall n-1.

Paired t test

$$t = \frac{Xbar_{diff}}{\left(\frac{sd_{diff}}{\sqrt{n}}\right)}$$

$Xbar_{diff}$ = Sample mean of the differences
sd_{diff} = standard deviation of differneces
n = sample size

degree of freedom, df = $n - 1$

4. Results and analysis

4.1 Accuracy of direct geo-referencing using raw onboard GPS data

The exterior orientation parameters of the UAV (sensor positions X; Y; Z, and orientation parameters x; u; j) can be obtained from the onboard GNSS and its attached IMU for each image at the time of exposure. The direct geo-referencing accuracy of a UAV system depends on the quality of its GPS receiver and IMU observations. Without using any GCPs, direct geo-referencing was performed, and all 10 GCPs were used as CPs to assess the accuracy. Table 2 shows the differences in coordinates between the GCPs and the photogrammetric solution showns.

C	D	E	F	G	H	I
	GCP		ORTHO		GE	
1	25.27661582	83.00149	25.27663	83.00154	25.27654	83.00146
2	25.27190254	82.99853	25.27195	82.99847	25.27192	82.99858
3	25.27283062	82.99157	25.27281	82.99158	25.27283	82.99161
4	25.27775998	82.98987	25.27781	82.98992	25.27777	82.98984
5	25.27484513	82.98933	25.27485	82.98931	25.2749	82.9894
6	25.26926044	82.98842	25.26927	82.98849	25.26926	82.98834
7	25.26590848	82.99559	25.26599	82.99554	25.257	82.9941
8	25.25667676	82.99413	25.25669	82.99418	25.25667	82.99417
9	25.26079377	79.01738	25.2608	79.0173	25.26078	79.01737
10	25.26814203	82.98741	25.26811	82.98737	25.26814	82.98731

Table 2:Shows the differences in the points with GCP ortho and Google Earth

							Diff			
UTM	GCP		ortho		GE		Ortho(X)	Y	GE(X)	Y
1	701541.47	2797081.1	701546.5	2797083	701538.6	2797073	-5.013	-1.646	2.896	8.444
2	701251.112	2796554.5	701245	2796560	701256.1	2796557	6.12	-5.057	-5.008	-2.009
3	700548.536	2796646.9	700549.6	2796645	700552.6	2796647	-1.041	2.269	-4.03	-0.008
4	700369.204	2797190.4	700374.2	2797196	700366.2	2797191	-4.954	-5.616	3.032	-0.622
5	700319.603	2796866.7	700317.6	2796867	700326.7	2796873	2.022	-0.51	-7.06	-6.296
6	700237.115	2796246.7	700244.1	2796248	700229.1	2796247	-7.034	-1.274	8.057	0.169
7	700964.855	2795886.1	700959.7	2795895	700976.1	2795873	5.173	-9.066	-11.275	12.96
8	700832.984	2794861.3	700838	2794863	700837	2794861	-5.015	-1.542	-4.038	0.567
9	699666.754	2795300.2	699674.8	2795301	699661.4	2795299	-8.072	-0.68	5.338	1.294
10	700137.216	2796121.3	700133.3	2796118	700127.3	2796121	3.878	3.495	9.869	0.36

Table:3 Shows the differences in the X and Y in the Ortho and Google Earth with respect to the GCP

4.2 Accuracy analysis by the statistical t-test result

The result analysis is also shown by the help of the mathematical statistical analysis with t-test is shown in the table and also the highest and lowest values of the differences is also shown by the tabulated form the X-ortho and Y-ortho of the images is shown

T-Test

Paired Samples Statistics

		Mean	N	Std. Deviation	Std. Error Mean
Pair 1	XGm	-.2219	10	7.01181	2.21733
	XOrtho	-1.3936	10	5.31728	1.68147

Paired Samples Correlations

		N	Correlation	Sig.
Pair 1	XGm & XOrtho	10	-.515	.127

Paired Samples Test

		Paired Differences					t	df	Sig. (2-tailed)
		Mean	Std. Deviation	Std. Error Mean	95% Confidence Interval of the Difference Lower	Upper			
Pair 1	XGm - XOrtho	1.17170	10.76413	3.40392	-6.52850	8.87190	.344	9	.739

Table4: The X points of the Ortho and Google Earth points and its analysis is done.

T-Test

[DataSet0]

Paired Samples Statistics

		Mean	N	Std. Deviation	Std. Error Mean
Pair 1	X1X2OrGm	-.8077	20	6.08629	1.36094
	Y1Y2OrGm	-.2384	20	4.85822	1.08633

Paired Samples Correlations

		N	Correlation	Sig.
Pair 1	X1X2OrGm & Y1Y2OrGm	20	-.130	.586

Paired Samples Test

		Paired Differences					t	df	Sig. (2-tailed)
		Mean	Std. Deviation	Std. Error Mean	95% Confidence Interval of the Difference Lower	Upper			
Pair 1	X1X2OrGm - Y1Y2OrGm	-.56935	8.26465	1.84803	-4.43732	3.29862	-.308	19	.761

Table5:The overall analysis of the Google Earth points with respect to the GCP's

T-Test

[DataSet0]

Paired Samples Statistics

		Mean	N	Std. Deviation	Std. Error Mean
Pair 1	XYOrtho	-1.6782	20	4.48189	1.00218
	XYGM	.6320	20	6.15789	1.37695

Paired Samples Correlations

		N	Correlation	Sig.
Pair 1	XYOrtho & XYGM	20	-.503	.024

Paired Samples Test

		Paired Differences					t	df	Sig. (2-tailed)
		Mean	Std. Deviation	Std. Error Mean	95% Confidence Interval of the Difference Lower	Upper			
Pair 1	XYOrtho - XYGM	-2.31015	9.26195	2.07104	-6.64488	2.02458	-1.115	19	.279

Table6: The overall analysis of the Ortho image points with respect to the GCP's

5. CONCLUSIONS

The overall analysis is done and shown in the mathematical form by the help of the T-test analysis which also helps in the 95% level of confidence checking which shows that the points which we were taken and its differences is shown by the help of ortho image and google earth points were differences were shown and its accuracy analysis is done by the statistical way which shows in the X and Y coordinates and its differences is shown in the above table.

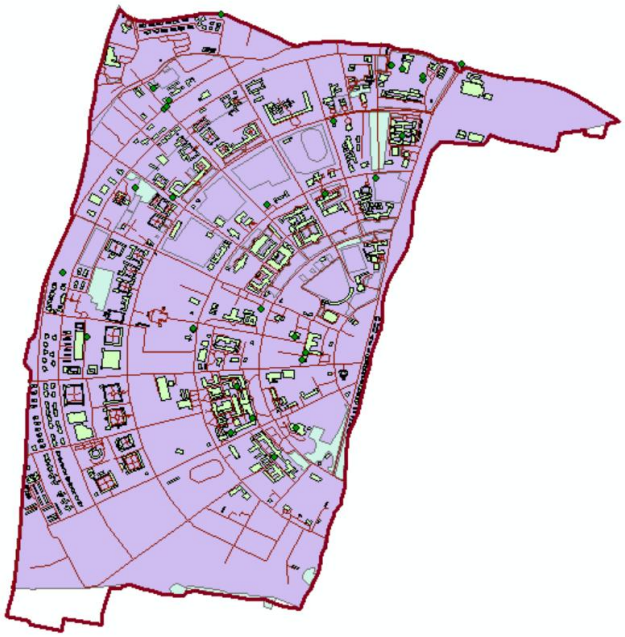

REFERENCES

1. A. Ansari, Use of point cloud with a low-cost UAV system for 3D mapping, 2012 International Conference on Emerging Trends in Electrical Engineering and Energy Management (ICETEEEM), IEEE, 2012, Doi: 10.1109/ iceteeem.2012.6494471

2. C. Cryderman, S.B. Mah, A. Shufletoski, Evaluation of UAV photogrammetric accuracy for mapping and earthworks computations, GEOMATICA 68 (4) (2014) 309–317, https:// doi.org/10.5623/cig2014-405.

3. D. Ebolese, M. Lo Brutto, G. Dardanelli, Uav survey for the archaeological map of LILYBAEUM (Marsala, Italy), ISPRS – Int. Arch. Photogrammetry, Remote Sens. Spatial Information.

4. D. Ekaso, F. Nex, N. Kerle, Accuracy assessment of real-time kinematics (RTK) measurements on unmanned aerial vehicles (UAV) for direct geo-referencing, Geo-Spatial Inf. Sci. 23 (2) (2020) 165–181, https://doi.org/10.1080/10095020.2019.1710437.

5. F. Marinello, A. Pezzuolo, D. Cillis, A. Chiumenti, L. Sartori, Traffic effects on soil compaction and sugar beet (Beta vulgaris L.) taproot quality parameters, Spanish J. Agricultural Res. 15 (1) (2017), https://doi.org/10.5424/sjar/2017151-8935 e0201.

6. F. Nex, F. Remondino, UAV for 3D mapping applications: a review, Appl. Geomatics 6 (1) (2013) 1–15, https://doi.org/ 10.1007/s12518-013-0120-x.

7. Elkhrachy, Modeling and visualization of three dimensional objects using low-cost terrestrial photogrammetry, Int. J. Arch. Heritage 14 (10) (2020) 1456–1467, https://doi.org/10.1080/ 15583058.2019.1613454.

8. J.-C. Padro´ , F.-J. Mun˜ oz, J. Planas, X. Pons, Comparison of four UAV georeferencing methods for environmental monitoring purposes focusing on the combined use with airborne and satellite remote sensing platforms, Int. J. Appl. Earth Obs. Geoinf. 75 (2019) 130–140, https://doi.org/10.1016/ j.jag.2018.10.018.

9. M. Gerke, H.J. Przybilla, Accuracy analysis of photogrammetric UAV image blocks: Influence of onboard RTK-GNSS and cross flight patterns, Photogrammetrie, Fernerkundung, Geoinformation 2016 (1) (2016) 17–30, https://doi.org/10.1127/ pfg/2016/0284.

10. M. Rabah, M. Basiouny, E. Ghanem, A. Elhadary, Using RTK and VRS in direct geo-referencing of the UAV imagery, NRIAGJ. Astron. Geophys. 7 (2) (2018) 220–226, https://doi.org/ 10.1016/j.nrjag.2018.05.003.

11. S. Siebert, J. Teizer, Mobile 3D mapping for surveying earthwork projects using an Unmanned Aerial Vehicle (UAV) system, Autom. Constr. 41 (2014) 1–14, https://doi.org/10.1016/ j.autcon.2014.01.004.

12. Y.-H. Tu, S. Phinn, K. Johansen, A. Robson, D. Wu, Optimising drone flight planning for measuring horticultural tree crop structure, ISPRS J. Photogramm. Remote Sens. 160 (2020) 83–96.